

## Translational to rotational energy transfer in molecule-surface collisions

Hailemariam Ambaye and J. R. Manson<sup>a)</sup>*Department of Physics and Astronomy, Clemson University, Clemson, South Carolina 29634*

(Received 23 January 2006; accepted 4 May 2006; published online 29 August 2006)

A theoretical approach that combines classical mechanics for treating translational and rotational degrees of freedom and quantum mechanics for describing the excitation of internal molecular modes is applied to the scattering of diatomic molecules from metal surfaces. Calculations are carried out for determining the extent of energy transfer to the rotational degrees of freedom of the projectile molecule. For the case of observed spectra of intensity versus final rotational energy, quantitative agreement with available experimental data for the scattering of NO and N<sub>2</sub> from close packed metal surfaces is obtained. It is shown that such measurements can be used to determine the average rotational energy of the incident molecular beam. Measurements of the exchange of energy between translational and rotational degrees of freedom upon collision are also described by calculations for these same systems. © 2006 American Institute of Physics.

[DOI: 10.1063/1.2209237]

### I. INTRODUCTION

The scattering of molecules from well-defined surfaces provides a direct way to study the interaction potential between a molecule and the surface and to discern the role of molecular internal degrees of freedom in this interaction. Such knowledge is a fundamental prerequisite for understanding important processes such as the transfer of energy between a gas and a surface as well as physisorption and chemisorption.<sup>1,2</sup>

Experimental results for such scattering processes are usually obtained by directing well-defined molecular jet beams at clean and well-ordered surface samples under ultrahigh vacuum conditions. The molecular velocities generated range typically from thermal to hypersonic speeds which roughly corresponds to translational energies of a few tens of meV up to several eV. The types of experimental measurements reported generally fall under four classes: (1) angular distributions in which the total scattered intensity summed over all translational energies and internal states is given as a function of final scattering angle, (2) translational energy-resolved spectra in which for fixed incident energy and beam angles the scattered intensity is reported as a function of final translational energy, (3) rotational spectra of the scattered intensity measured as a function of final rotational energy, and (4) probabilities for excitation of internal molecular vibrational modes.

There is also a distinction made between the scattering of small mass molecules such as H<sub>2</sub> and large mass molecules typified by atmospheric gases such as O<sub>2</sub>, N<sub>2</sub>, CO, and NO. This distinction arises because hydrogen and its similar small-mass isotopic molecular combinations exhibit pronounced quantum mechanical effects such as diffraction in the angular distributions as well as single phonon excitation and small quantum number rotational excitation in the energy-resolved spectra.<sup>3</sup> In particular, the energies of rota-

tional excitational quanta of hydrogenic molecules are large compared to those of the atmospheric diatomic gases. On the other hand, the heavier gases even at relatively small translational energies in the thermal range tend to create large numbers of phonons upon collision with the surface and similarly the rotational quantum numbers of the scattered molecules tend to be large, both effects indicating that the translational and rotational spectra of these molecules may be reasonably described by classical mechanics.

The purpose of this paper is to present a series of calculations describing the surface collisions of large-mass diatomic molecules using a theory that describes the translational and rotational motions with classical mechanics. Previous work using the same theoretical approach has concentrated on descriptions of the angular distributions<sup>4,5</sup> and translational energy resolved spectra of diatomic and small polyatomic molecules.<sup>6,7</sup> In this paper the emphasis is on describing the effects of excitation of the rotational energy of the molecule.

One standard way of reporting rotational excitation in molecular scattering experiments is to show the intensity probability as a function of final rotational energy.<sup>8-15</sup> Often such a plot will be analyzed in terms of a Maxwell-Boltzmann distribution of scattered rotational energies using the effective temperature as an adjustable parameter. Sometimes such a fitting procedure is pushed further and the effective final rotational temperature is examined as a function of other experimentally controllable parameters such as translational energy and angle of the incident beam or surface temperature. It is clear that the scattering process cannot be generally described by Boltzmann equilibrium conditions, as evidenced by the fact that the derived effective rotational temperatures depend on the detector angle and have little relationship to the surface temperatures; however, such analysis has been very useful in the past. It is shown here in several examples that the rotational intensity spectra can be explained by a relatively straightforward classical excitation

<sup>a)</sup>Electronic mail: jmanson@clemson.edu

theory without recourse to an adjustable effective final rotational temperature. However, in several cases the theoretical results can be compared to previously obtained effective rotational temperatures and the general dependence on surface temperature and incident energy is well reproduced. A further interesting result is obtained from an examination of the intensity spectra at relatively small rotational energies. It is shown that a comparison of measurements with calculations can give important information about the rotational state of the incident molecular beam.

Another frequently presented way of exhibiting experimental results for molecular scattering is to examine the relationship of translational energy to rotational energy, usually in the form of plots of average final translational versus rotational energy.<sup>9,10,16</sup> This can be a rather complicated relationship because energy can also be exchanged with the molecular internal vibrational modes or with the surface phonons or electron-hole pair excitations. However, the simplest arguments based on energy conservation between rotational and translational motion would predict a negative correlation between the two, i.e., those scattered molecules with the highest rotational energies should on average have less translational energy, and this is what is generally observed. We show here that these observations are in agreement with classical theoretical predictions.

An important question that must be addressed is the role of internal molecular vibrational modes. For the diatomic molecules considered here the excitation energy of the stretch modes is typically of the order of 200 meV or larger, relatively large compared to incident beam energies. This has important consequences; in particular, it implies that only small quantum numbers will be excited implying that the theoretical description must be quantum mechanical. However, it also implies, as is verified both by direct measurements<sup>17,18</sup> and by our present calculations, that the internal mode excitation probabilities are small. Our calculations indicate that the effect of internal mode excitation on the rotational and translational energy transfers is negligible for all of the experimental cases considered here.

The theoretical model is the same that has been used previously to analyze molecular scattering angular distributions,<sup>4,19</sup> translational energy resolved scattered intensity spectra,<sup>6,7</sup> and final rotational temperatures in the case of C<sub>2</sub>H<sub>2</sub> scattering from LiF(001).<sup>8,20</sup> The translational and rotational motions are treated classically in a manner that retains the conservation laws for energy, translational momentum parallel to the surface and angular momentum perpendicular to the surface. The other components of linear and angular momentum are not conserved because of the broken symmetry in the direction perpendicular to the surface. However, because typical internal molecular vibrational modes can be large compared to the translational energies involved in the experiments to be analyzed here, these vibrational excitations are treated quantum mechanically with a generalized forced-oscillator model. This model depends on the interaction potential through a multiplicative form factor  $|\tau_{fi}|^2$  which is the square of a transition matrix. As in previous work<sup>4,6,7</sup> we use the semiclassical limit for a potential in which the surface barrier term is represented by a flat, hard

repulsion where the matrix element is given by  $|\tau_{fi}| \rightarrow 2p_{fz}p_{iz}/m$  where  $p_{fz}$  and  $p_{iz}$  are the perpendicular components of the final and initial momentum. The theory also depends on a velocity parameter<sup>21,22</sup>  $v_R$  which we choose to be 1000 m/s although the results, since they involve mainly rotational excitations, are not strongly affected by its value.

The final operation necessary for comparing the state-to-state transition rates to experimental data is to average over all quantities not measured by the experiment. Since the incident molecular jet beam has a distribution of rotational states approximating an equilibrium distribution at small temperature, an average is taken over an incident Boltzmann distribution of rotational energies, as well as an average over classical rotational orientations. The excitation of internal degrees of freedom depends on the orientation of the angular momentum vector both before and after collision, so the results must also be averaged over relative orientation angles.

The organization of this paper is as follows. Section II shows a comparison of the calculated results with experimental measurements for the intensity spectra as functions of final rotational energy. Section III is a discussion of a series of comparisons of theory with measurements for the relationship between translational and rotational energy transfers in the scattered molecules. Discussion and some conclusions are given in Sec. IV.

## II. ROTATIONAL INTENSITY SPECTRA

In the late 1970s laser induced fluorescence detection was developed into a tool that was capable of measuring the internal state distributions of molecules scattered from surfaces.<sup>23–25</sup> Several examples of such spectra for the scattering of NO by Ag(111) are shown in Fig. 1 in which the scattered intensity with the detector in the scattering plane and positioned at the specular angle ( $\theta_f = \theta_i$ ) is plotted as a function of final rotational energy in a semilogarithmic graph.<sup>9,10</sup> In Fig. 1(a) the surface temperature for all measurements was 650 K; the upper three sets of data were measured at an angle  $\theta_i = 15^\circ$  with three different incident translational energies,<sup>9</sup> 1000 meV (open circles), 750 meV (filled circles), and 320 meV (open diamonds); the fourth data set (filled diamonds) was taken for  $E_i^T = 320$  meV and  $\theta_i = 40^\circ$ . Figure 1(b) shows a second set of measurements for the same system taken by the same group at a later date. All those measurements were for  $\theta_i = 15^\circ$  and three different energies and temperatures:  $E_i^T = 850$  meV and  $T_S = 273$  K (open squares),  $E_i^T = 850$  meV and  $T_S = 520$  K (filled squares), and  $E_i^T = 90$  meV and  $T_S = 520$  K (open triangles).<sup>10</sup> The intensities are presented in arbitrary units, and for clarity the various data sets are separated by arbitrary constant amounts.

These experimental measurements exhibit several evident characteristics; the intensity decreases strongly with increasing rotational energy and there is a steep initial decrease for small  $E_f^R$  followed by a large range of  $E_f^R$  for which the intensity decreases nearly exponentially (i.e., nearly a straight line in the logarithmic plot). For some of the measurements, in particular, for those taken at higher incident beam energies, there is a second pronounced decrease in intensity for very large  $E_f^R$ . This high rotational energy feature

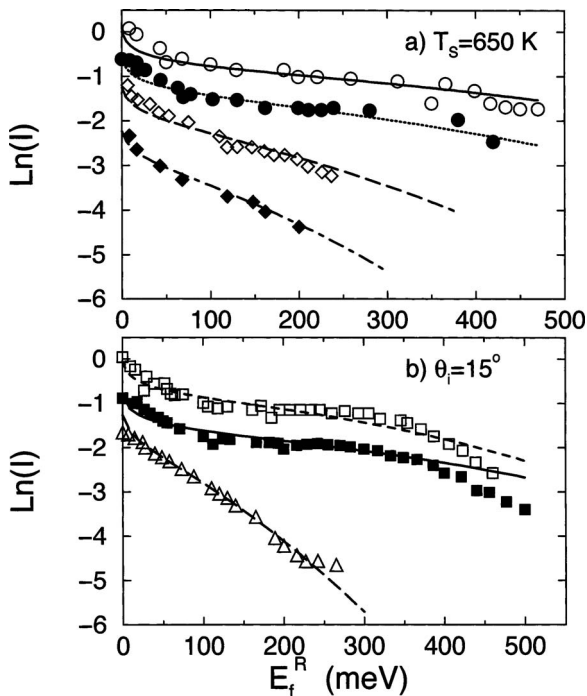


FIG. 1. Final rotational energy resolved intensity at specular scattering angles for several incident energies and surface temperatures. (a) Data taken from Ref. 9:  $T_s=650$  K; open circles are data for  $E_i=1000$  meV and  $\theta_i=15^\circ$ , solid circles are data for  $E_i=750$  meV and  $\theta_i=15^\circ$ , open diamonds are data for  $E_i=320$  meV and  $\theta_i=15^\circ$ , and solid diamonds are data for  $E_i=320$  meV and  $\theta_i=40^\circ$ . (b) Data taken from Ref. 10.  $\theta_i=15^\circ$ ; open squares are data for  $E_i=850$  meV and  $T_s=273$  K, solid squares are data for  $E_i=850$  meV and  $T_s=520$  K, and triangles are data for  $E_i=90$  meV and  $T_s=520$  K. Curves are calculations.

is termed the rotational rainbow and it arises because there is a classical limit on the amount of angular momentum that can be transferred to a molecule in a single collision. Quantum mechanics allows for larger transfers of angular momentum but typically only with sharply reduced probabilities beyond the classical limit.

Also shown in Fig. 1 are calculated curves. For each final rotational energy these calculations are the sum of the differential reflection coefficient over the internal vibrational stretch mode excitations, final translational energies, and an average is carried out over all possible molecular orientations. The differential reflection coefficient is also averaged over an assumed Maxwell-Boltzmann distribution of initial rotational states with a temperature  $T_R=35$  K which is in approximate agreement with experimental conditions.<sup>9</sup> A distribution of incident molecular vibrational frequencies at a temperature of 125 K, somewhat larger than the rotational temperature, is also assumed in agreement with estimated experimental conditions. The calculations were found to depend only weakly on the distribution of initial rotational states as long as the average rotational energy was small compared to the incident translational energy, and this is discussed further in connection with Fig. 8 below.

Relatively good quantitative agreement is seen between calculations and experiment. The initial steep decline in intensity is somewhat overemphasized by the calculations, but it occurs over the same energy range as the observations. The long plateau of exponential decay for intermediate energies

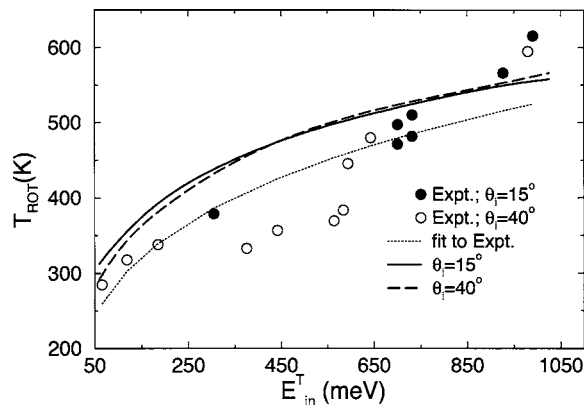


FIG. 2. Normal incident energy dependence of the final rotational temperature for specular scattering at  $T_s=650$  K. Solid and long dash curves are theory for  $\theta_i=15^\circ$  and  $40^\circ$ , respectively. Solid circles are data for  $\theta_i=15^\circ$ , and open circles are data for  $\theta_i=40^\circ$ . The dotted curve is a least squares fit to the experimental data. Data are taken from Ref. 9.

is well matched. The calculations do not reproduce the rotational rainbow behavior observed at higher incident energies, but this is understandable because the simple interaction potential used to calculate the scattering form factor does not include the possibility of a rainbow. The data of Fig. 1(a) have in an earlier study been analyzed using molecular dynamics simulations that included a relatively sophisticated interaction potential energy surface.<sup>15</sup> This study obtained a good description of the experimental data and, in particular, obtained a correct prediction of the rotational rainbow. The present work demonstrates that most of the observed features, with the exception of the rotational rainbow, are not strongly dependent on details of the potential energy landscape but instead arise largely from the statistical mechanics of the scattering process.

A traditional way of analyzing rotational energy spectra data such as that shown Fig. 1 is to compare each curve to a Maxwell-Boltzmann distribution with an effective rotational temperature  $T_{ROT}$ . This kind of analysis is suggested by the large range of  $E_f^R$  values for which the intensity is nearly exponential. Figure 2 exhibits such an analysis, plotting experimental rotational temperatures  $T_{ROT}$  as a function of incident normal energy  $E_{in}^T=E_i^T \cos^2(\theta_i)$  for conditions similar to those of Fig. 1(a) with a surface temperature of 650 K and two incident angles of  $15^\circ$  and  $40^\circ$  as shown.<sup>9</sup> In order to obtain the experimental values for the effective rotational temperatures, straight lines were fitted to the data in the energy range of  $0 < E_f^R < 60$  meV, and a standard deviation of 25 K was reported. The dotted line shown in Fig. 2 is a least squares fit to the experimental data.

Also shown in Fig. 2 are two calculations, a solid curve for  $\theta_i=15^\circ$  and a dashed curve for  $\theta_i=40^\circ$ . The experimental data do not appear to depend strongly on incident angle, and the two calculations which are quite similar confirm this behavior. The effective rotational temperature  $T_{ROT}$  increases rather strongly with incident energy and this behavior is qualitatively explained by the calculations. However, it must be emphasized that the whole concept of finding an effective rotational temperature is simply a convenient fitting procedure, because it is clear that the scattering does not give rise

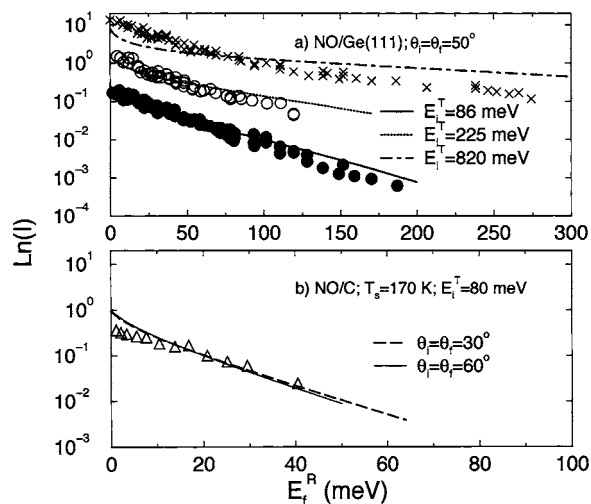


FIG. 3. Final rotational energy resolved intensity for specular scattering geometry. (a) NO/Ge(111) for  $T_S=800$  K and  $\theta_i=50^\circ$ . The times symbols are data at  $E_i=825$  meV, open circles are data for  $E_i=225$  meV, and solid circles are data for  $E_i=86$  meV. Data are from Ref. 11. (b) NO scattering from graphite for  $T_S=170$  K and  $E_i=80$  meV.  $\theta_i=30^\circ$  and  $60^\circ$  as marked. Data are from Ref. 12.

to anything approaching equilibrium behavior in the rotational spectra of the scattered beam. This is evidenced by the fact that  $T_{ROT}$  has a dependence on the incident translational energy, that it deviates significantly from the surface temperature, and also the original spectra such as in Fig. 1 exhibit substantial deviations from purely exponential equilibrium behavior.

The molecule of choice for many of the experiments measuring rotational energy spectra has been NO and two more examples appear in Figs. 3 and 4. Figure 3(a) gives data for NO scattering from Ge(111) at a temperature  $T_S=800$  K,  $\theta_i=\theta_f=50^\circ$ , and for the three incident translational energies of 86 meV (filled circles), 225 meV (open circles), and 820 meV (x symbols),<sup>11</sup> while Fig. 3(b) shows a single set of data taken by the same group for NO scattering from a graphite surface with  $T_S=170$  K and an incident energy of 80 meV.<sup>12</sup> The data were taken for two different specular configurations,  $\theta_i=\theta_f=30^\circ$  and  $60^\circ$ , and little difference was

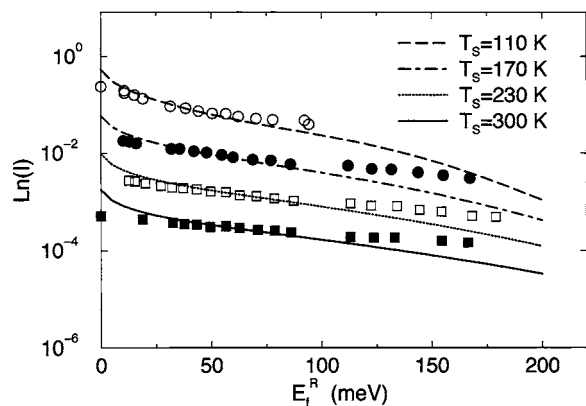


FIG. 4. Final rotational energy resolved intensity at  $\theta_i=20^\circ$  and incident energy  $E_i=352$  meV for specular scattering of NO from a Pt(111) substrate covered with 0.5 ML of CO. Open circles are data for  $T_S=110$  K, solid circles are data for  $T_S=170$  K, open squares are data for  $T_S=230$  K, and solid squares are data for  $T_S=300$  K. Data are from Ref. 13.

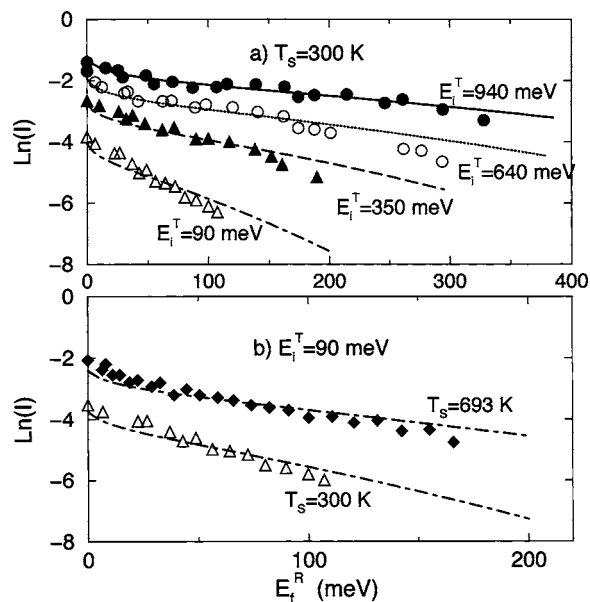


FIG. 5. The final rotational energy distribution under specular geometry conditions for several incident energies and surface temperatures for  $N_2/Cu(110)$ . (a)  $T_S=300$  K;  $E_i=90, 350, 640,$  and  $940$  meV as marked. (b)  $E_i=90$  meV;  $T_S=300$  K and  $T_S=693$  K. Symbols are experimental data from Ref. 14, and curves are theory.

noted between the two sets of measurements. Calculated curves at both angles are given in Fig. 3(b) and they also predict very little difference in the two configurations.

A quite different surface is exhibited in Fig. 4 which shows four spectra measured for NO scattering from a Pt(111) surface with a 0.5 ML coverage of CO. The incident energy is 352 meV,  $\theta_i=\theta_f=20^\circ$ , and the four different temperatures are 110, 170, 230, and 300 K as marked.<sup>13</sup> The calculated curves exhibited for each set of experimental data were carried out with the same parameters (incident rotational temperature,  $v_R$ , and  $\omega_R$ ) as for those shown in Fig. 1. Again these calculations are seen to agree reasonably well with the measurements.

A more recent and quite extensive experimental examination of a different system,  $N_2$  scattering from Cu(110), is shown in the rotational energy spectra of Fig. 5. These measurements cover a range of incident beam translational energies from 90 to 1000 meV and surface temperatures from 100 to 700 K as marked, and the measurements were made for incident and final angles nearly normal to the surface.<sup>14</sup> Each of these sets of experimental points is compared to calculations carried out with the same incident beam parameters as in the previous graphs. In this case the calculated curves agree quantitatively with the measurement for the whole rotational energy range except in some cases for the highest energy points measured. The experimental points at small  $E_f^R$  values for most incident conditions display the rather sharp decrease exhibited in the calculations, but at large  $E_f^R$  there is little indication of rotational rainbow cutoff behavior.

Much of the data for the  $N_2/Cu(110)$  system was presented in terms of the dependence of the effective final rotational temperature on the incident energy and surface temperature, and this is shown in Figs. 6 and 7. The dependence

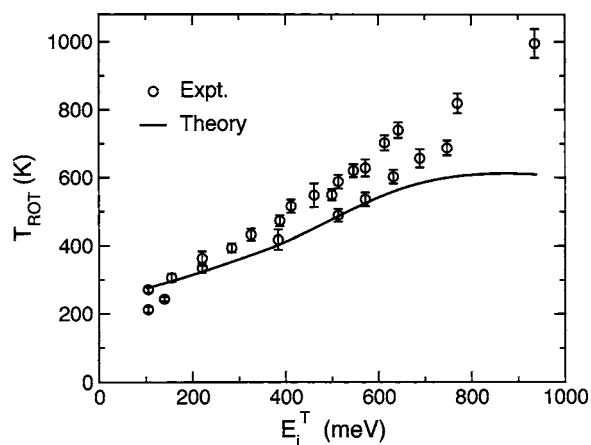


FIG. 6. The rotational temperature as a function of incident energy for  $N_2/Cu(110)$ . Symbols are experimental data from Ref. 14, and the curve is theory.  $T_S=300$  K and  $\theta_i=\theta_f=0^\circ$ .

on incident energy is in Fig. 6 for a surface temperature of 300 K. The measurements indicate a nearly linearly increasing behavior with  $T_{ROT}$  ranging from a value of about 200 K which is less than the surface temperature for  $E_i^T=90$  meV to values of  $T_{ROT}\approx 1000$  K at the highest energies of nearly 1 eV. Our calculations agree qualitatively with this increasing  $T_{ROT}$  except near the highest incident energies where the calculations show less increase. The dependence of  $T_{ROT}$  on surface temperature is shown in Fig. 7 for two different incident energies, 90 and 350 meV. The effective rotational temperature increases monotonically with temperature, and relatively good predictions of this behavior is given by the calculations. However, there is very little indication that the effective rotational temperature has anything more than a very weak relationship to the equilibrium surface temperature.

One interesting point that arises from the comparisons of calculations with the rotational energy spectra data is that, for nearly all incident conditions reported, the calculations show a very sharp decrease at small rotational energy, and this decrease is observed in much of the available data. However, all available data were obtained using molecular jet

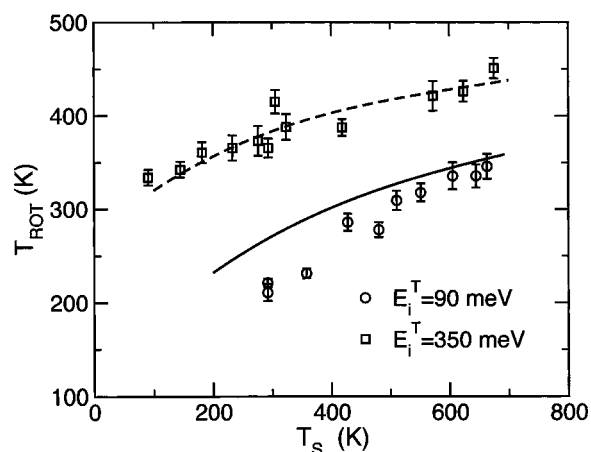


FIG. 7. The final rotational temperature as a function of surface temperature for  $N_2/Cu(110)$  at  $E_i^T=90$  and 350 meV. Symbols are experimental data from Ref. 14, and curves are theory.  $\theta_i=\theta_f=0^\circ$ .

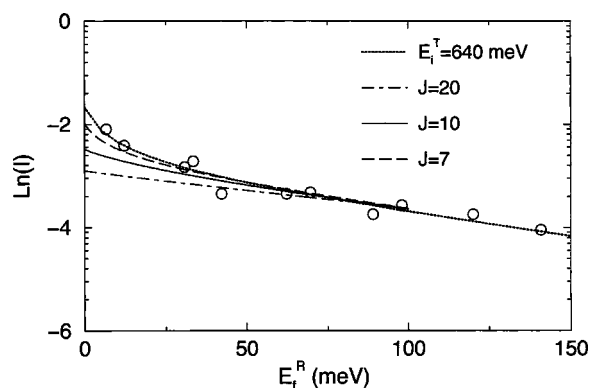


FIG. 8. The final rotational energy distribution for  $E_i^T=640$  meV and surface temperature of 300 K for  $N_2/Cu(110)$ . Symbols are experimental data from Ref. 14, the dash curve is theory with a cold initial rotational distribution of  $T_R=35$  K, the long dash curve is theory with initial rotational state with  $E_i^R=13.4$  meV ( $J=7$ ), solid curve is theory with initial rotational state at 26.4 meV ( $J=10$ ), and dot dashed curve is theory with initial rotational state at 100.8 meV ( $J=20$ ).  $\theta_i=\theta_f=0^\circ$ .

beams which are known to produce very cold rotational distributions, typically of a few tens of kelvins, and are relatively independent of translational energy. Our calculations indicate that the low  $E_f^R$  energy behavior is due to the cold incident rotational distribution and that if an incident beam with a rotational energy distribution comparable to the translational energy were used the effect would disappear. This is demonstrated in Fig. 8 which shows several calculations compared to the  $N_2/Cu(110)$  data for  $E_i^T=640$  meV and  $T_S=300$  K from Fig. 5. The dotted curve is the same calculation shown in Fig. 5 for an incident beam with a rotational temperature of 35 K. The dashed curve shows a calculation not for a Boltzmann distribution of rotations but for a beam with a single rotational energy of 13.4 meV for all  $N_2$  molecules. This energy would correspond approximately to the  $J=7$  rotational quantum level. It is clear that the sharp decrease at low rotational energy is somewhat damped but the behavior at large  $E_f^R$  is essentially unchanged.

The solid curve in Fig. 8 is for an incident beam having a fixed rotational energy of 26.4 meV (approximately the same as the  $J=10$  rotational state) and it is seen that the low energy decrease is significantly reduced. For the dash-dotted curve, the rotational energy is fixed at 100.8 meV, about the same as that for the  $J=20$  quantum level, and the calculated rotational energy spectrum becomes nearly exponential over the entire energy range. However, all curves regardless of initial rotational state saturate to nearly the same behavior at large  $E_f^R$ . Thus, it appears clear that the anomalous behavior of the rotational energy spectra at small  $E_f^R$  is due to the cold rotational distribution of the incident beam. Although we did not show in Fig. 8 the calculations that average over incident Boltzmann rotational distributions with very high temperatures, our calculations show that the effect is similar and that for high incident rotational temperatures the effect tends to disappear. This, in fact, could become a very useful effect. It indicates that careful measurements of the small  $E_f^R$  behavior of the spectra, when compared with calculations such as those presented here, can be used to determine the rotational energy distribution of the incident beam.

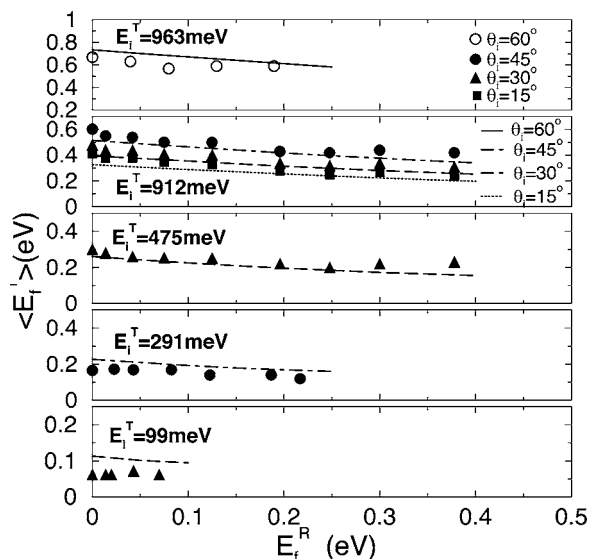


FIG. 9. Final average translational energy as a function of final rotational energy for several incident energies and angles taken at the specular scattering angle for NO scattering from Ag(111). In each panel the experiment and theory for a given incident energy and angle are compared. Open circles are data at  $\theta_i=60^\circ$ , solid circles are data at  $45^\circ$ , solid triangles are data at  $30^\circ$ , and solid squares are data at  $15^\circ$ . Calculations are the curves in each panel.  $T_s=450$  K and  $v_R=1000$  m/s. Data are taken from Ref. 10.

### III. DEPENDENCE OF FINAL TRANSLATIONAL ENERGY ON ROTATIONAL ENERGY

In addition to the rotational energy spectra discussed in the above section a number of experimental studies have made direct measurements of the exchange of translational energy to rotational energy,<sup>26–29</sup> often presented as plots of the scattered average translational energy  $\langle E_f^T \rangle$  as a function of rotational energy  $E_f^R$ . These plots generally show a negative correlation, that is to say, the average translational energy tends to decrease with increasing rotational energy. Intuitively, such behavior would be suggested by the law of conservation of energy as applied to these two degrees of freedom, but this is not completely valid because there is always the possibility of energy transfer to and from the surface and the internal vibrational modes.

We would like to discuss here two of these experiments for the same systems for which rotational energy spectra were discussed in Figs. 1 and 5. A series of graphs of  $\langle E_f^T \rangle$  vs  $E_f^R$  is shown in Fig. 9 for NO scattering from Ag(111).<sup>10</sup> The surface temperature is 450 K, incident translational energies range from 99 to 963 meV, and the measurements were made under specular conditions with incident angles ranging from  $15^\circ$  to  $60^\circ$  as marked. In all cases except for the lowest energy incident beam, the average final energy decreases by 10%–20% over the range of measured final rotational energies, which in some cases extends to as large as 400 meV. Our calculations, shown as curves, also reproduce this same behavior rather well except for the lowest energy.

The data shown in Fig. 9 have also been analyzed previously using molecular dynamics calculations<sup>15</sup> and the same interaction potential surface mentioned in Sec. II above.<sup>16</sup> The results were quite similar to those obtained here.

The case of the low energy  $E_i^T=99$  meV beam requires further examination. As opposed to the higher energy measurements, there is essentially no decrease in measured average final energy as  $E_f^R$  increases and the final energy is about 60% of the incident energy. This would indicate that a large fraction of the incident translational energy is transferred to the surface lattice and relatively little is being converted to molecular rotational energy. The theoretical calculations, on the other hand, predict a 10% decrease over the measured  $E_f^R$  energy range, and additionally they predict an average final translational energy that is larger than the incident energy rather than smaller as measured. The most likely explanation for this discrepancy is the effect of an attractive physisorption well which is not present in the calculations. The adsorption well increases the incident energy of the molecule while at the same time refracting it to a more normal incidence trajectory, and both effects tend to cause a larger energy loss to the surface. We have carried out additional calculations for this case in which an adsorption well was modeled by an attractive square well, a reasonable approximation that produces the refraction effect. However, the effect of such a physisorption well of depth of 50 meV, and even larger, was to reduce the calculated average final translational energy only by about 10 meV which is not enough to bring it into agreement with measured values.

Another effect that occurs at low incident energies is that the differential reflection coefficient, which gives the intensity versus final translational energy spectrum, becomes skewed towards relatively larger intensities at higher final energies. For large incident energies the intensity spectrum as a function of final energy is a nearly symmetric, Gaussian-like function for which the most probable and average final energies are nearly equal. At low incident energies and especially for high surface temperatures, the intensity spectra become skewed towards higher energies and the average final energy is larger than the most probable energy. For the case of the  $E_i^T=99$  meV beam in Fig. 9 the most probable energy is calculated to be nearly 40 meV smaller than the average energy.

A second example<sup>14</sup> that exhibits the relation between translational and rotational energies for the case of  $N_2$  scattering from Cu(110) is shown in Fig. 10. The filled circles show experimental data at two widely different incident energies for the most probable final translational energy<sup>30</sup> denoted as  $\langle E_f^T \rangle$  plotted as a function of  $E_f^R$ . The surface temperature is 300 K and the incident beam and detector directions are near normal, the same conditions as in Fig. 5. Also shown as open circles is the sum of translational and rotational energies given by

$$E_f^{TR} = \frac{\langle E_f^T \rangle + E_f^R}{E_i^T}. \quad (1)$$

Again, as in Fig. 9 the most probable final energy decreases monotonically with  $E_f^R$ . Interestingly, however, the sum of translational and rotational energies of Eq. (1) is an increasing function. In fact, at the lower incident energy of 90 meV this sum actually becomes larger than the incident translational energy which, given that the internal modes of the

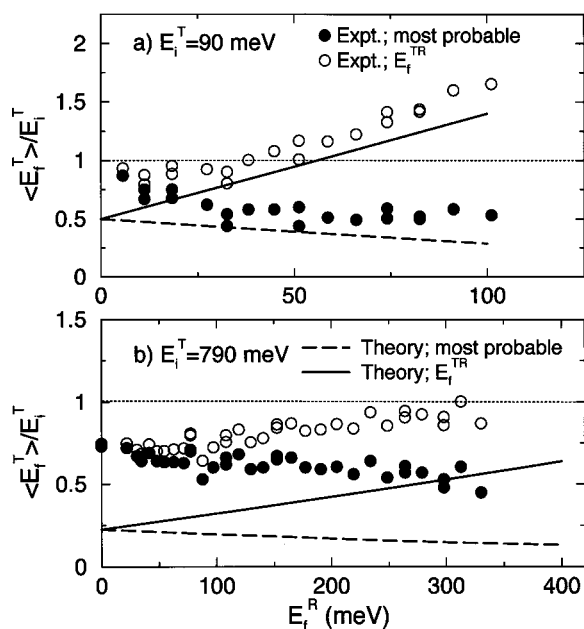


FIG. 10. The normalized most probable translational energy  $\langle E_f^T \rangle / E_i^T$  and the sum of the most probable and the rotational energy  $E_f^{TR} = (\langle E_f^T \rangle + E_f^R) / E_i^T$  as functions of the final rotational energy for two incident energies. (a)  $E_i^T = 90$  meV and (b)  $E_i^T = 790$  meV. Symbols are experimental data from Ref. 14, and lines are theory.  $T_S = 300$  K and  $\theta_i = \theta_f = 0^\circ$ .

incident molecule are not strongly excited, would imply that energy in the scattered beam is being gained from the surface phonon modes. It also implies that there exists a recovery energy, which is the value of the final rotational energy for which  $E_f^{TR} = 1$ , i.e., the point at which the most probable plus rotational energies equal the incident energy.

Calculations of  $\langle E_f^T \rangle$  and  $E_f^{TR}$  are also shown in Fig. 10. The calculated results for both quantities as functions of  $E_f^R$  are essentially straight lines with nearly the same slope as that of the experimental points. However, the calculated absolute values are substantially smaller than the measured values. If the experimental data is extrapolated back to  $E_f^R = 0$  it indicates that for both cases only about 25% of the incident energy is lost upon collision. However, the calculated values give about 50% energy loss for  $E_i^T = 90$  meV and about 75% loss at  $E_i^T = 790$  meV. The calculated energy losses, at least for the 790 meV beam, are comparable to the value of 75% obtained from a crude estimate assuming a pseudoatomic two body collision between a particle having the mass of  $N_2$  colliding with a single stationary Cu atom, i.e., the Baule estimate.

The reason for this discrepancy between calculation and experiment in the translational energy loss to the surface could be due to collective effects in the collision; i.e., the incoming  $N_2$  molecule may be effectively colliding with more than one Cu atom. An estimate of such a collective effect can be obtained by carrying out a calculation with an effective mass larger than that of a single Cu atom. Such a calculation is given in Fig. 11 in which the same experimental data are compared to a calculation similar to that of Fig. 10 except that an effective substrate mass of seven times the mass of a single Cu atom is used. This brings the calculation into much better agreement with experiment, especially for

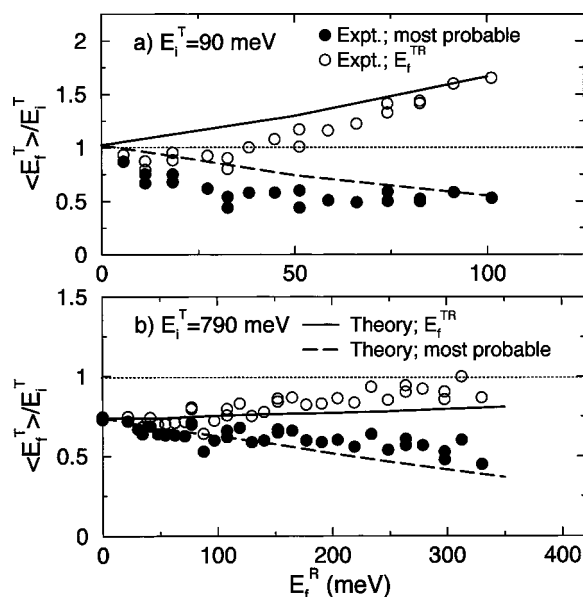


FIG. 11. Same as Fig. 10 except with calculations for an effective surface mass of  $7M_{Cu}$ .

the higher incident energy case. However, it is not clear why an effective mass is necessary to obtain agreement for the  $N_2/Cu(110)$  case but not for  $NO/Ag(111)$ .

#### IV. DISCUSSION AND CONCLUSIONS

In this paper we have investigated the interplay between translational and rotational degrees of freedom in the collision of a molecule with a surface. In particular, we wished to determine if a theory based on classical mechanics for translational and rotational motion can correctly predict the exchange of energy between these two degrees of freedom and with the surface. Although modern experimental methods are capable of resolving molecular rotational states to very large quantum numbers the major features of the scattering process, and, in particular, the energy transfers, appear to be determined by the envelope of the observed multiquantum scattering spectra for the cases investigated here, which involve diatomic molecules with masses an order of magnitude larger than  $H_2$  and translational energies in the thermal range or greater.

The theory used is a straightforward approach that depends on relatively little input about the interaction potentials but properly accounts for the conservation laws for energy as well as linear and angular momenta and includes a proper treatment of the statistical mechanics involved in the collision process. In addition to classical treatments of translational and rotational degrees of freedom, the internal molecular vibrational modes are treated with semiclassical quantum mechanics and the scattering probability for a single collision process with the surface can be expressed in closed form. The relatively good agreement obtained in comparisons of theoretical calculations with experimental measurements indicates that much of the information obtained in the energy transfer process between rotational and translational degrees of freedom is controlled by the statistical mechanics and the general conservation laws.

The specific results considered here are descriptions of two types of experiments. The first consists of measurements of rotational intensity spectra in which the scattered intensity is measured as a function of final rotational energy, and the second are average or most probable final energies measured as functions of the final rotational energy. Relatively good explanations of the experimental measurements are obtained for both cases. There have been previous calculations that have also obtained good agreement with some of these same data,<sup>15,16</sup> and these calculations were based on molecular dynamics simulations. The present approach, because it is based on theoretical expressions that can be written in closed form, has the ability to predict the qualitative behavior of the response of the scattering system to experimentally controllable parameters without carrying out extensive numerical calculations.

Several important observations arise from this work. The first concerns the question of internal molecular vibrational modes and their importance in the scattering process. Our results indicate that for molecules such as those studied here with large vibrational excitation energies the internal vibrational modes are unimportant in the transfer of energy between translational and rotational degrees of freedom. This conclusion was verified by carrying out independent calculations with rigid molecule models.

The measured and calculated scattered spectra considered here are clearly nonequilibrium in nature. However, there is a widespread tradition of analyzing aspects of the experimental data by comparing the measured scattered spectra to Maxwell-Boltzmann distribution functions. In particular, this is the case for the rotational intensity spectra. We show here that such analysis has its limits but can be a useful way of tabulating the behavior of the scattering process as functions of the experimentally controlled parameters and also for comparison with more detailed scattering theory.

When measurements are reported for spectra that are not state to state, i.e., results that are averaged over many states such as the average final translational energy, it is important to specify precisely what has been measured. An example arising during the course of this work is that the average and most probable final translational energies can be quite different. This is especially true for low energy incident beams colliding with hot surfaces, cases for which the scattered distribution may appear as a highly skewed broad peak. In such situations only the average final translational energy can determine whether total translational energy has been gained or lost by the particles in the collision process.

An important practical result to arise from this work is the recognition that the small rotational energy behavior of the rotational intensity spectra can provide important information about the rotational state of the incident molecular beam. A recurring signature of the observed intensity versus final rotational energy spectra is a sharp decrease in intensity

at small final rotational energies. We show that this sharp decrease is due to the typically very cold rotational state of the incident molecular jet beams. Thus, the rotational intensity spectra can, when compared with a theory such as that used here, give the rotational distribution of the incident beam.

## ACKNOWLEDGMENT

This work was supported by the Department of Energy under Grant No. DE-FG02-98ER45704.

- <sup>1</sup> *Atomic and Molecular Beam Methods*, edited by G. Scoles (Oxford University Press, Oxford, 1988).
- <sup>2</sup> *Atomic and Molecular Beams: State of the Art 2000*, edited by R. Campargue (Springer, Heidelberg, 2001).
- <sup>3</sup> A recent example of work on D<sub>2</sub> scattering from LiF, together with extensive references to earlier literature, appears in Y. Ekinici and J. P. Toennies, *Phys. Rev. B* **72**, 205430 (2005).
- <sup>4</sup> H. Ambaye, J. R. Manson, O. Weiße, C. Wesenberg, M. Binetti, and E. Hasselbrink, *J. Chem. Phys.* **121**, 1901 (2004).
- <sup>5</sup> T. Kondo, T. Sasaki, and S. Yamamoto, *J. Chem. Phys.* **116**, 7673 (2002); T. Tomii, T. Kondo, T. Hiraoka, T. Ikeuchi, S. Yagyu, and S. Yamamoto, *ibid.* **112**, 9052 (2000); T. Kondo, T. Tomii, T. Hiraoka, T. Ikeuchi, S. Yagyu, and S. Yamamoto, *ibid.* **112**, 9940 (2000).
- <sup>6</sup> I. Moroz and J. R. Manson, *Phys. Rev. B* **69**, 205406 (2004).
- <sup>7</sup> I. Moroz and J. R. Manson, *Phys. Rev. B* **71**, 113405 (2005).
- <sup>8</sup> T. W. Francisco, N. Camillone III, and R. E. Miller, *Phys. Rev. Lett.* **77**, 1402 (1996).
- <sup>9</sup> A. W. Kleyn, A. C. Luntz, and D. J. Auerbach, *Phys. Rev. Lett.* **47**, 1169 (1981).
- <sup>10</sup> C. T. Rettner, J. Kimman, and D. J. Auerbach, *J. Chem. Phys.* **94**, 734 (1991).
- <sup>11</sup> A. Mödl, H. Robota, J. Segner, W. Vielhaber, M. C. Lin, and G. Ertl, *J. Chem. Phys.* **83**, 4800 (1985).
- <sup>12</sup> F. Frenkel, J. Häger, W. Krieger, H. Walther, G. Ertl, J. Segner, and W. Vielhaber, *Chem. Phys. Lett.* **90**, 225 (1982).
- <sup>13</sup> M. K. Ainsworth, V. Fiorin, M. R. S. McCoustra, and M. A. Chesters, *Surf. Sci.* **433–435**, 790 (1999).
- <sup>14</sup> J. L. W. Siders and G. O. Sitz, *J. Chem. Phys.* **101**, 6264 (1994).
- <sup>15</sup> C. W. Muhlhausen, L. R. Williams, and J. C. Tully, *J. Chem. Phys.* **83**, 2594 (1985).
- <sup>16</sup> J. Kimman, C. T. Rettner, D. J. Auerbach, J. A. Barker, and J. C. Tully, *Phys. Rev. Lett.* **57**, 2053 (1986).
- <sup>17</sup> C. T. Rettner, F. Fabre, J. Kimman, and D. J. Auerbach, *Phys. Rev. Lett.* **55**, 1904 (1985).
- <sup>18</sup> C. T. Rettner, J. Kimman, F. Fabre, D. J. Auerbach, J. A. Barker, and J. C. Tully, *J. Vac. Sci. Technol. A* **5**, 508 (1987).
- <sup>19</sup> I. Iftimia and J. R. Manson, *Phys. Rev. A* **87**, 093201 (2001).
- <sup>20</sup> I. Iftimia and J. R. Manson, *Phys. Rev. B* **65**, 125412 (2002).
- <sup>21</sup> R. Brako and D. M. Newns, *Phys. Rev. Lett.* **48**, 1859 (1982); R. Brako, *Surf. Sci.* **123**, 439 (1982).
- <sup>22</sup> H.-D. Meyer and R. D. Levine, *Chem. Phys.* **85**, 189 (1984).
- <sup>23</sup> G. Pruett and R. N. Zare, *J. Chem. Phys.* **64**, 1774 (1976).
- <sup>24</sup> P. Andersen and A. C. Luntz, *J. Chem. Phys.* **72**, 5842 (1980).
- <sup>25</sup> J. L. Kinsey, *Annu. Rev. Phys. Chem.* **28**, 349 (1977).
- <sup>26</sup> H. Mortensen, E. Jensen, L. Diekhöner, A. Baurichter, A. C. Luntz, and V. V. Perunin, *J. Chem. Phys.* **118**, 11200 (2003).
- <sup>27</sup> G. O. Sitz, A. C. Kummel, and R. N. Zare, *J. Chem. Phys.* **89**, 2558 (1988); **89**, 2572 (1988); **89**, 6947 (1988).
- <sup>28</sup> K. C. Janda, J. E. Hurst, J. P. Cowin, L. Wharton, and D. J. Auerbach, *Surf. Sci.* **130**, 395 (1983).
- <sup>29</sup> F. Buddle, A. Mödle, A. V. Hamza, P. M. Ferm, and G. Ertl, *Surf. Sci.* **192**, 507 (1987).
- <sup>30</sup> G. O. Sitz (private communication).